Dynamics of the Heterogeneous Electron-Transfer Reaction of Cytochrome C 552 from Thermus Thermophilus, a Time-Resolved Surface-Enhanced Resonance Raman Spectroscopic Study

ARTICLE *in* THE JOURNAL OF PHYSICAL CHEMISTRY B · OCTOBER 1999

Impact Factor: 3.3 · DOI: 10.1021/jp991818d

3 AUTHORS, INCLUDING:

Sophie Lecomte
Université Bordeaux 1
78 PUBLICATIONS **1,123** CITATIONS
SEE PROFILE

Tewfik Soulimane
University of Limerick
116 PUBLICATIONS **2,406** CITATIONS
SEE PROFILE

Dynamics of the Heterogeneous Electron-Transfer Reaction of Cytochrome c_{552} from *Thermus thermophilus.* A Time-Resolved Surface-Enhanced Resonance Raman Spectroscopic Study

Sophie Lecomte,*,† Peter Hildebrandt,*,‡ and Tewfik Soulimane§

Laboratoire de Dynamique, Interactions et Réactivité UPR-1580, CNRS−Université Paris VI, 2 rue Henry Dunant, F-94320 Thiais, France, Max-Planck-Institut für Strahlenchemie, Stiftstrasse34-36, D-45470 Mülheim, Germany, and Institut für Biochemie, Klinikum Aachen, Pauwelsstrasse 30, D-52057 Aachen, Germany

Received: June 3, 1999; In Final Form: August 18, 1999

The heterogeneous electron-transfer process of cytochrome c_{552} (Cyt-c_{552}) adsorbed on an Ag electrode was studied by surface-enhanced resonance Raman (SERR) spectroscopy. Upon adsorption the heme protein Cyt-c_{552}, which acts as an electron carrier in the respiratory chain of *Thermus thermophilus*, exists in a potential-dependent equilibrium between two conformational states (B1, B2) similar to cytochrome *c* (Cyt-*c*) (Wackerbarth et al. *Appl. Spectrosc.* **1999**, *53*, 283). From the stationary SERR spectra measured as a function of the potential, the apparent redox potential of state B1 was determined to be −0.044 V (versus saturated calomel electrode) which is 31 mV more negative than the redox potential of Cyt-c_{552} in solution. On the basis of a model for the interfacial potential distribution that accounts for the potential drop at the redox site of the adsorbed protein, it is concluded that the true redox potential of the adsorbed state B1 is the same as that for the heme protein in solution. This conclusion is consistent with the structural identity of state B1 and Cyt-c_{552} in solution that is derived from the comparison of the SERR and resonance Raman spectra. On the other hand, the formation of B2 is associated with substantial structural changes of the heme pocket and a large negative shift of the redox potential. The dynamics of the heterogeneous reduction of B1 was studied by time-resolved SERR spectroscopy which combines the spectroscopic measurements with the potential jump technique. In contrast to Cyt-*c*, the electron transfer was found to be much faster than the conformational transition to B2 so that the data could be analyzed on the basis of a one-step relaxation process. For the formal unimolecular electron-transfer rate constant a value of 4.6 s^{-1} was obtained. On the basis of the rate constants measured as a function of the overpotential, the reorganization energy was determined to be 0.15 eV. This unusually low value may be due to a strongly diminished contribution of the solvent reorientation for the adsorbed species and the specific heme pocket structure of Cyt-c_{552} optimized for the electron-transfer reaction. The differences in the electron-transfer mechanism and dynamics compared to Cyt-*c* are obviously related to the unique structural properties of Cyt-c_{552} which may be the consequence of the adaptation to the extreme living conditions of the thermophilic bacterium.

Introduction

For a large number of redox proteins, electron transfer (ET) to their natural reaction partners occur over long distances of more than 10 Å.[1] Most of these reactions take place at charged interfaces constituted by anionic and cationic binding domains of the partner proteins. Typical examples are the reduction processes of cytochrome *c* oxidase (CcO) and cytochrome *c* peroxidase by cytochrome *c* (Cyt-*c*).[2] These long-range ET reactions require the involvement of amino acids to provide (specific) ET pathways. Furthermore, the electron has to be transferred across the electrical double layer of the protein−protein interface.

Most of the information about long-range ET reactions are obtained from photoinduced ET processes of metalloproteins in which additional photoactive redox sites are covalently attached to amino acids on the protein surface.[3] However, in these reactions the electron is not transferred along the natural pathway that is used for the interprotein ET. Thus, the kinetic parameters derived from these studies are only of limited value for characterizing the biological process. This is particularly true for the reorganization energy which has to be corrected for the large contributions from the artificial solvent exposed redox site. Furthermore, this approach fails to consider the effect of the charged protein−protein interface on the ET process in an adequate manner.[4]

Such drawbacks can be overcome by studying ET processes of these redox proteins at electrodes.[5] In the past years, considerable progress has been made in the development of electrochemical techniques as well as in the preparation of coated electrodes so that the determination of unimolecular heterogeneous rate constants of heme proteins is possible.[6−10] Reorganization energies determined in electrochemical experiments exclusively refer to the natural redox site of the heme protein and the molecular environment and are in fact substantially smaller than those derived from photoinduced ET reactions of labeled proteins.[3,8,9] Furthermore, appropriate choice of the electrochemical system generally allows the interaction of the

* To whom correspondence should be addressed.
† CNRS−Université Paris VI.
‡ Max-Planck-Institut für Strahlenchemie.
§ Klinikum Aachem.

10.1021/jp991818d CCC: $18.00
Published on Web 10/27/1999

redox protein with the electrode via the natural binding domain[5] so that the ET is likely to follow the same pathway as that in the biological reaction.

On the other hand, electrochemical techniques do not provide any structural information about the interfacial processes and, hence, are not appropriate to elucidate the mechanism of complex redox processes that may include additional reactions of the electroactive species coming before or after the ET. These are, for instance, conformational transitions of the redox protein that are induced by the electrostatic interactions in the electrical double layer of the electrode/electrolyte interface and that may also occur upon complex formation with the natural redox partners.[11] This has indeed been shown for Cyt-*c* which undergoes the same structural changes upon binding to electrodes as well as to CcO.[11−13] These conformational transitions may be of functional relevance for the biological ET providing a high efficiency and unidirectionality for the electron flow to the oxidase.[13c] Analogous processes may constitute the molecular basis also for conformationally gated ET of other redox couples as suggested from kinetic studies in solution.[14] Consequently, a comprehensive analysis of the interfacial redox process requires the identification of intermediate species and the determination of their dynamics.

Surface-enhanced Raman (SER) spectroscopy is a technique which can fulfill these requirements.[15] Because of the selective enhancement of the Raman scattering upon adsorption on electrochemically roughened metal (Ag, Au, Cu) electrodes, it can be used to probe the molecular structure exclusive of the species in the electrical double layer. This technique has successfully been employed to study the potential-dependent equilibria of heme proteins where the SER effect and the molecular resonance Raman (RR) effect can be combined (surface-enhanced resonance Raman, SERR).[12,16−19] Under these conditions, the sensitivity is further increased and the measured spectra exclusively display the vibrational bands of the heme group (i.e., the redox center) of the adsorbed protein. Furthermore, SERR spectroscopy has recently been extended to the time-resolved domain by combining the SERR spectroscopic measurements with the potential-jump technique. Thus, it is possible to probe the dynamics of the interfacial processes of heme proteins in the millisecond time scale.[20,21]

In this work we have carried out a systematic stationary and time-resolved SERR spectroscopic analysis of the interfacial redox process of cytochrome c_{552} (Cyt-c_{552}) in continuation of our previous studies.[19,20] Cyt-c_{552} is a mobile electron carrier in the respiratory chain of *Thermus thermophilus* where it transfers electrons to the terminal membrane-bound ba_3-oxidase.[22] This heme protein exhibits some unique structural and functional properties which differ from those of other soluble *c*-type cytochromes.[23] Cyt-c_{552} lacks the typical lysine-rich cluster on the front surface that in Cyt-*c* serves as a binding domain for the reaction partner.[2] Instead, the region around the exposed heme edge is shielded by an additional more unpolar peptide segment which is suggested to increase the thermostability of the protein.[23] Hence, interactions with the ba_3-oxidase may be qualitatively different compared to other eukaryotic and prokaryotic Cyt-*c*/CcO redox couples and may account for the high specificity of the Cyt-c_{552}/ba_3-oxidase reaction.[22−25] Thus, a detailed analysis of the interfacial redox process of Cyt-c_{552}, which is the goal of the present study, promises to elucidate the differences and similarities of the biological electron-transfer mechanism compared to Cyt-*c*.

Materials and Methods

Cyt-c_{552} was isolated and purified as described previously.[22,23] For RR and SERR spectroscopic experiments, the samples were dissolved in 10 mM Tris-HCl buffer (pH 7.0) with a final protein concentration of 15 and 0.1 μM, respectively. For the SERR experiments, the samples also include 50 mM KCl as a supporting electrolyte.

RR and SERR spectra were measured with 413-nm cw-excitation of a Kr-ion laser with a power of ca. 50 mW at the sample. The spectra were recorded with a spectrograph (U1000, ISA) equipped with a liquid-nitrogen-cooled CCD camera. The spectral resolution was 2.5 cm^{-1} and the wavenumber increment per data point was 0.5 cm^{-1}. The SERR spectra were measured with a rotating Ag cylinder electrode using a three-electrode cell controlled by a potentiostat. All potentials cited in this work refer to the saturated calomel electrode (SCE). The preparation of SER-active surfaces followed the protocol described previously.[21] For time-resolved SERR experiments, a rapid potential jump was applied to the working electrode to perturb the equilibrium of the adsorbed species and the SERR signals were measured at a delay time δ subsequent to the potential jump. Following the measuring event, the potential was reset to the initial value so that the original equilibrium could be restored. An opto-mechanical device synchronized the sequences of potential jumps and measuring intervals Δt which were repeated until a satisfactory signal-to-noise ratio was achieved. The experimental setup and the principles of the time-resolved experiments are described in detail elsewhere.[21]

Stationary and time-resolved SERR spectra were repeated several times under the same conditions to ensure reproducibility. The total (effective) accumulation time for each experiment was 20 and 3 s for the stationary and time-resolved experiments, respectively. To improve the signal-to-noise (S/N) ratio, the individual spectra were combined only if their difference spectra yield straight lines. Prior to the spectra analysis, the structureless background was removed by polynomial subtraction. The spectra obtained in this way were analyzed by a band fitting or a component analysis.[26]

Results

Conformational Equilibria of the Adsorbed Cyt-c_{552}. The SERR spectra of Cyt-c_{552} that are obtained from a rotating and nonrotating electrode at −0.4 and 0.0 V are shown in Figure 1. SERR spectra of that quality could only be measured when KCl was used as a supporting electrolyte. In contrast to Cyt-*c*, much less intense signals were obtained upon replacement of KCl by Na_2SO_4.[12,21] The spectra displayed in Figure 1 show the marker band region including the modes whose frequencies are characteristic for the oxidation, ligation, and spin state of the heme iron.[27] At −0.4 V, the adsorbed Cyt-c_{552} is expected to be exclusively in the reduced form which is in fact confirmed by the position of the oxidation marker band ν_4 at ca. 1360 cm^{-1} in the spectra obtained either with the rotating or the nonrotating electrode (Figure 1B,A). These two devices, however, yield substantially different spectra at 0.0 V (Figure 1C,D). When a rotating electrode is used, the resultant SERR spectrum includes an appreciable portion of the reduced form as indicated by the distinct shoulder at 1360 cm^{-1} adjacent to the prominent band at 1372 cm^{-1} (Figure 1C). Without the electrode being rotated, the oxidized species is clearly the dominant form (Figure 1D).[19] Furthermore, the spectrum obtained with this device reveals significant changes also in the region above 1450 cm^{-1}, which for example, includes new bands at 1491 and 1628 cm^{-1}. These bands, which are characteristic of a five-coordinated (5c)

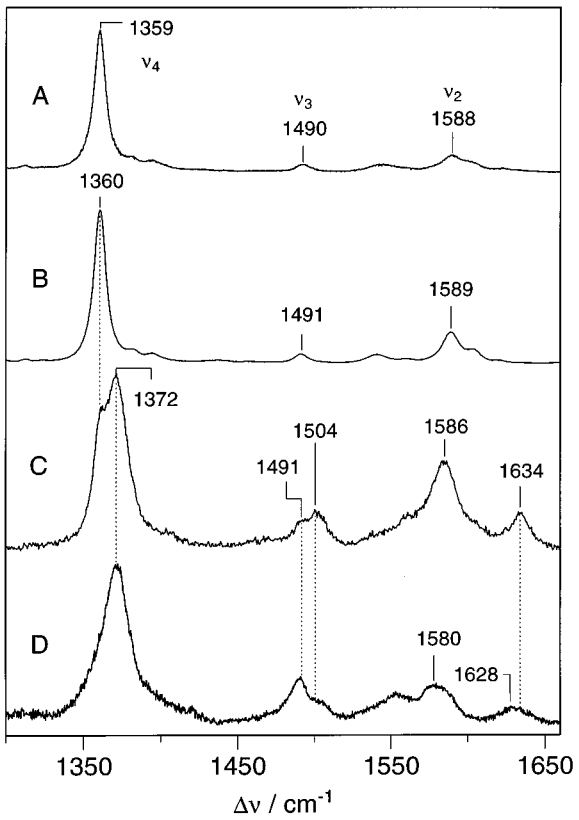

Figure 1. SERR spectra of Cyt-c_{552} measured with 413-nm excitation: (A) nonrotating electrode at −0.4 V; (B) rotating electrode at −0.2 V; (C) rotating electrode at 0.0 V; (D) nonrotating electrode at 0.0 V. Further experimental conditions are given in the text.

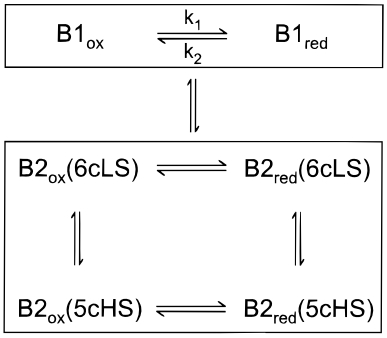

Figure 2. Scheme for the redox and conformational equilibria of the adsorbed Cyt-c_{552}.

high-spin (HS) species,[27] are much weaker in the spectrum obtained with the rotating electrode. Evidently, there are also new bands in the spectrum of Figure 1D which contribute to the broadening of the peaks at ca. 1550 and 1580 cm^{-1}. Such a broadening, albeit not so pronounced, is also revealed by a careful inspection of the corresponding spectrum measured at −0.4 V (Figure 1A). All these spectral changes are fully reversible upon variation of the potential, implying that they do not reflect a denaturation of the adsorbed protein. These results are reminiscent of previous findings for the adsorbed mitochondrial Cyt-*c* which has been shown to exist in a conformational equilibrium between two states, i.e., state B1 which exhibits essentially the same spectrum as the dissolved Cyt-*c* and state B2 which comprises a five-coordinated high-spin (5cHS) and a new six-coordinated low-spin (6cLS) form.[12] Therefore, it is very likely that also the adsorbed Cyt-c_{552} exists in a similar conformational equilibrium (Figure 2).[19,20] Then the differences between the spectra obtained with a rotating and a nonrotating electrode reflect different equilibrium distributions between the various species. These changes of the equilibrium concentrations can be attributed to local heating of the adsorbed molecules in the laser focus which is significantly stronger for a nonrotating electrode than for a rotating electrode.[21]

Determination of the Component Spectra of the Adsorbed Cyt-c_{552}. The conformational equilibria of the adsorbed Cyt-c_{552} depend on the potential so that relative contributions of the individual species to the spectra could easily be varied by a change in the potential. Thus, a global component analysis[26] of the SERR spectra measured at various potentials allows one to determine the pure spectra of the individual species. In this analysis, *i*-measured spectra, M_i, are fitted by a set of complete component spectra, N_j, of the species *j* which are supposed to be involved according to the scheme in Figure 2. Thus, for all measured spectra, the relationship

$$M_i = \sum_j g_{ij} N_j \qquad (1)$$

holds. The underlying assumption of this approach is that the component spectra N_j are potential-independent and only their relative amplitudes g_{ij} vary in the various measured spectra.

Initial component spectra for the conformational state B2 required for the global fitting procedure were obtained by mutual subtraction of some of those measured spectra.[19,26] Also, the previous results for Cyt-*c* served as a guideline for constructing the initial spectra.[12] Only the component spectrum of the reduced state B1 ($B1_{red}$) could be measured directly without interference from the contributions of other species using the rotating electrode at potentials <-0.2 V (cf. Figure 1B). The spectra measured between −0.2 and −0.4 V reveal no indication for any structural heterogeneity. Furthermore, the spectral parameters of the reduced B1 were found to be invariant in this potential range, supporting the assumption that the component spectra of all species can be regarded as potential-independent.

In addition, the analysis of the spectrum of $B1_{red}$ reveals far-reaching similarities to that of the RR spectrum of the reduced form of the dissolved Cyt-c_{552} so that it is reasonable to assume that this spectral identity also holds for the oxidized form.[12,19] Therefore, the component spectrum of the oxidized state B1 ($B1_{ox}$), which could not be measured directly, was regarded as being identical to the oxidized form of the dissolved protein. In contrast to Cyt-*c*,[12] the measured spectra reveal no indication for a HS species of the reduced state B2, which should exhibit a characteristic marker band at ca. 1470 cm^{-1}. Therefore, the global analysis of the experimental spectra M_i measured at different potentials with a rotating and a nonrotating electrode was carried out on the basis of five-component spectra whereas three of them [$B2_{ox}$(6cLS), $B2_{ox}$(5cHS), $B2_{red}$(6cLS)] were iteratively refined during the fitting procedure. Note that in this fitting procedure the degrees of freedom are restricted to the number of components, providing a substantially higher reliability of the results than those of conventional band fitting.[26] In fact, a good global fit for five components was achieved, which a posteriori supports the validity of the proposed scheme in Figure 2.

Finally, the pure spectra of all individual species were obtained by a weighted subtraction of the measured spectra according to

$$N_k = \sum_i \frac{(M_i - \sum_{j \neq k} g_{ij} N_j)}{g_{ik}} \qquad (2)$$

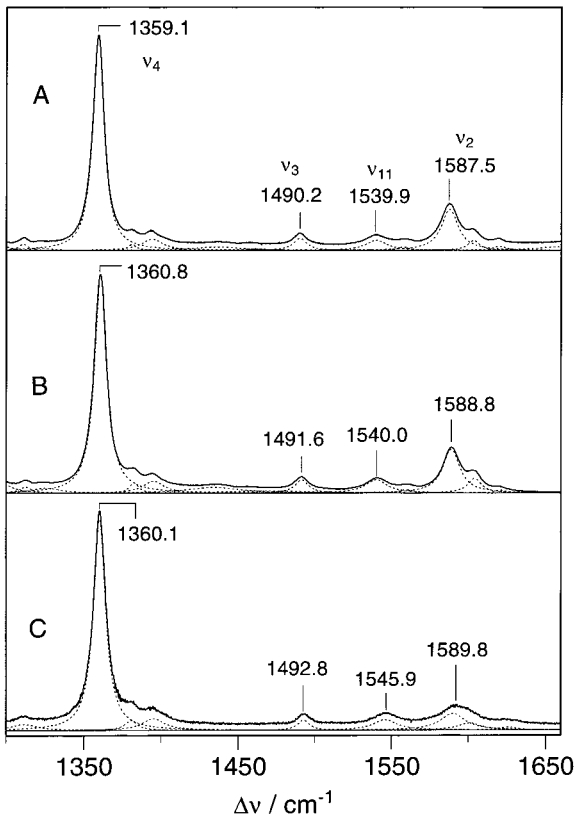

Figure 3. SERR spectra of reduced species of state B1 (B) and B2 (C) of the adsorbed Cyt-c_{552} as determined from the component analysis, compared with (A) the RR spectrum of the dissolved (chemically) reduced Cyt-c_{552}. The excitation wavelength was 413 nm. Further experimental conditions are given in the text. The dotted lines indicate the fitted Lorentzian band shapes.

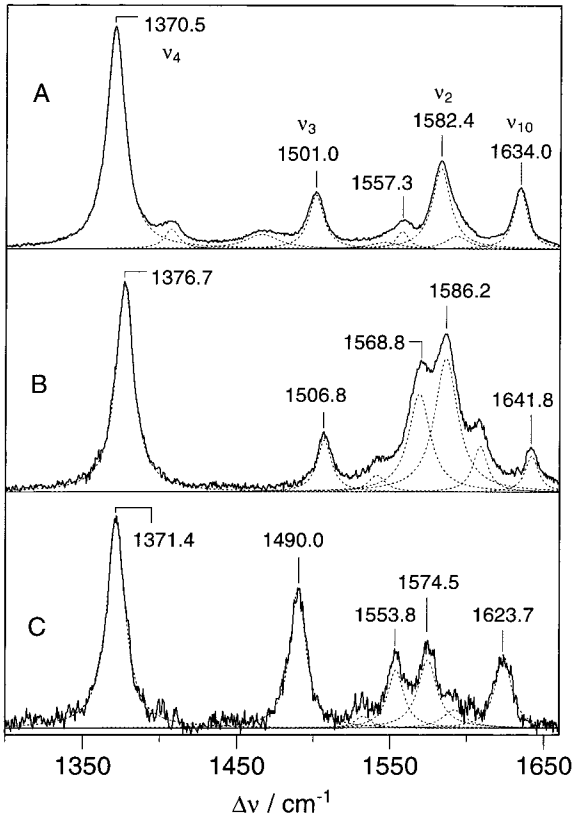

Figure 4. SERR spectra of the oxidized species of the adsorbed Cyt-c_{552} as determined from the component analysis: (A) state B1; (B) 6cLS form of state B2; (C) 5cHS form of state B2. The excitation wavelength was 413 nm. Further experimental conditions are given in the text. The dotted lines indicate the fitted Lorentzian band shapes.

These spectra are shown in Figures 3 and 4 and the spectral parameters are listed in Table 1. The accuracy of the quantitative analysis depends on the spectral differences between the various species.[26] These differences are quite pronounced for $B1_{red}$, $B1_{ox}$, $B2_{ox}$(6cLS), and $B2_{ox}$(5cHS), whereas the component spectrum of $B2_{red}$(6cLS) is similar to that of $B1_{red}$. However, the $B2_{red}$(6cLS) species is not formed in the potential range from 0.0 to −0.25 V studied in this work, so that the quantitative analysis of the spectra is substantially facilitated.

Determination of the Redox Potential. The component analysis allows the quantitative determination of the relative contribution of each species to the measured SERR spectra (cf. eq 1). Thus, it is possible to analyze the potential dependence of the conformational and redox equilibria of the adsorbed Cyt-c_{552}. It was found that the conformational state B2 (oxidized species) is formed at more positive potentials, i.e., > -0.05 V, whereas at potentials < -0.05 V state B1 dominates. The findings are again similar to those for Cyt-*c*.[12]

To analyze the redox equilibria of the adsorbed Cyt-c_{552} quantitatively, potential-dependent SERR spectra were measured in 10- to 20-mV increments in the range of the putative redox potential. For state B1, the redox potential was expected to be close to that of the dissolved species (−0.013 V)[29] so that SERR spectra were measured between −0.1 V and +0.05 V (Figure 5). In fact, these SERR spectra reveal that upon a decrease in the potential the contribution of the reduced B1 increases at the expense of the oxidized B1. Note that the spectra also include small contributions of the oxidized state B2 which in turn increases substantially at potentials greater than −0.01 V. The relative contributions of $B1_{red}$ and $B1_{ox}$ to the measured spectra

TABLE 1: Spectral Parameters of the Marker Bands of the Various Species of Cyt-c_{552}[a]

mode[b]	$B1_{red}$	$B2_{red}$	$B1_{ox}$	$B2_{oxLS}$	$B2_{oxHS}$
ν_4	1360.8	1360.1	1370.5	1376.7	1371.4
	(1.000)	(1.000)	(1.000)	(1.000)	(1.000)
ν_3	1491.6	1492.8	1501.0	1506.8	1490.0
	(0.061)	(0.048)	(0.246)	(0.249)	(0.667)
ν_{11}	1540.0	1545.9	1557.3	1568.8	1553.8
	(0.061)	(0.049)	(0.080)	(0.474)	(0.278)
ν_{38}	1559.4		1546.0	1541.1	1532.4
	(0.015)		(0.030)	(0.081)	(0.057)
ν_2	1588.8	1589.8	1582.4	1586.2	1574.5
	(0.020)	(0.078)	(0.367)	(0.647)	(0.324)
ν_{37}	1604.0	1600.9	1592.8	1608.4	1591.8
	(0.067)	(0.033)	(0.058)	(0.221)	(0.086)
ν_{10}	1620.9	1626.0	1634.0	1641.8	1623.7
	(0.013)	(0.014)	(0.274)	(0.174)	(0.351)

[a] Frequencies are given in cm^{-1}; relative intensities (in parentheses) refer to the mode ν_4. [b] Assignments and notation according to Hu et al.[28]

that were determined by the component analysis, i.e., the relative intensities I_j (corresponding to $g_{ij}N_j$; see eq 1), are related to the relative concentrations c_j of the species j according to

$$c_j = f_j I_j \tag{3}$$

so that the Nernst equation is then given by

$$E = E^0 - \frac{RT}{nF} \ln \frac{f_{B1(red)} I_{B1(red)}}{f_{B1(ox)} I_{B1(ox)}} \tag{4}$$

where E^0 is the redox potential of the adsorbed species, n is the

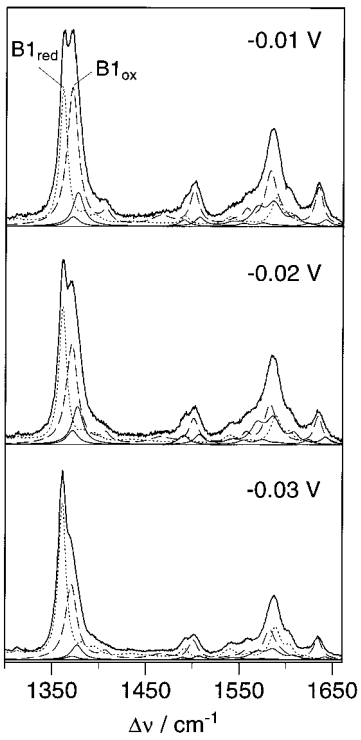

Figure 5. SERR spectra of the adsorbed Cyt-c_{552} measured at different potentials. The excitation wavelength was 413 nm. Further experimental conditions are given in the text. The dotted and dashed lines indicate the component spectra of the reduced and oxidized form of state B1, respectively. The solid lines indicate the 6cLS and 5cHS forms of the oxidized state B2.

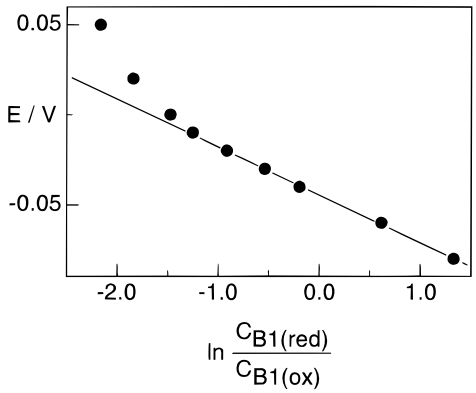

Figure 6. Nernstian plot for the redox process of B1 according to eq 4. The data were determined from the SERR spectra as described in the text.

number of transferred electrons, and R, T, and F have the usual meaning. The ratio of the proportionality factors f_i can be determined from the RR spectra of the reduced and oxidized Cyt-c_{552} in solution, yielding a value of 0.2825.[19] This approximation is justified in view of the spectral similarity of B1 and the dissolved Cyt-c_{552}. Then, the concentration ratios of $B1_{red}$ and $B1_{ox}$ are plotted semilogarithmically versus the potential (Figure 6).

Between -0.01 and -0.08 V the data follow a straight line with a correlation coefficient of 0.9997. The slope yields a value of 0.94 for a number of transferred electrons, which is close to the theoretical value for a one-electron redox couple. The redox potential is determined to be -0.044 V, which is somewhat more negative than that of the dissolved Cyt-c_{552} (-0.013 V).[29] However, Figure 6 reveals notable deviations from linearity at potentials > -0.01 V, which can be ascribed to the effect of the charge redistribution in the electrical double layer upon approaching the oxidation potential of Ag/AgCl (see below).

Attempts to apply a corresponding analysis to the redox equilibrium of state B2 failed because in the range of the expected redox potential (-0.3 V to -0.4 V) the equilibrium concentrations of B2 are very small because of the rapid conversion to $B1_{red}$. For this reason, also, the time-resolved SERR studies had to be restricted to the redox process of the conformational state B1.

Time-Resolved SERR Experiments of State B1. For the time-resolved SERR measurements, Cyt-c_{552} was adsorbed at -0.4 V to ensure that the protein was exclusively in state B1 as checked by a stationary SERR experiment. Subsequently, the potential was set to the initial potential E_i to start the time-resolved experiments. The initial dwell time at E_i (ca. 5 s) was sufficiently long to establish the redox equilibrium of B1. After each time-resolved experiment, a stationary SERR spectrum was measured at -0.4 V. Except for a slight lowering of the total intensity, these spectra reveal no differences compared to those measured prior to the time-resolved experiments. Thus, any denaturation processes of the adsorbed Cyt-c_{552} can be ruled out.

The ranges of the potential jumps were chosen according to the following criteria: (i) large differences between the equilibrium concentrations of $B1_{red}/B1_{ox}$ at the initial and the final potentials, E_i and E_f, which are essential for a reliable quantitative analysis of the time-resolved SERR spectra; (ii) large variations of the potential difference ΔE between E_f and E^0 (i.e., the overpotential that determines the driving force for the ET), which are required for the determination of the reorganization energy. Because of the oxidation potential of Ag/AgCl and the concomitant loss of SERR activity at potentials close to E^0(Ag/AgCl), a value of 0.0 V constitutes the upper limit for the accessible potentials. For the heterogeneous oxidation this value corresponds to a maximum ΔE of only -0.044 V, which is not sufficient for determining the reorganization energy. Hence, the time-resolved SERR experiments were restricted to the reduction of the adsorbed Cyt-c_{552}. Consequently, E_f was varied from $E_f = E^0$ ($\Delta E = 0$ V) to negative values to increase the driving force for the heterogeneous reduction whereas E_i was confined to the range between 0.0 V and E^0 (-0.044 V).

Upon increase of the driving force, the processes to be monitored became faster so that a continuous improvement of the time resolution was required. With the present experimental setup, this could be achieved by increasing the rotational speed of the chopper wheel which in turn, however, reduced the recovery time for the initial equilibrium.[21] Thus, eventually the dwell time at E_i became too small to guarantee the "fresh-sample" condition, leading to steady-state distributions between the reduced and the oxidized B1. It was found that this limit was reached at final potentials < -0.22 V, corresponding to overpotentials ΔE ($= E_f - E^0$) < -0.176 V. Note that up to this limit the ET process is still much slower than the relaxation time of the double layer.[20,21]

Figures 7 and 8 show a selection of time-resolved SERR spectra measured at various delay times for two different potential jumps. As expected, the reduced B1 increases at the expense of $B1_{ox}$ with increasing delay times. On the other hand, the contribution of the oxidized B2 (6cLS and 5cHS) is small and does not vary with the delay time. These results confirm previous conclusions that the conformational transition $B1_{ox} \rightarrow B2_{ox}$ is much slower than the ET of B1.[20] Thus, the data analysis could be restricted to the ET process based on a one-step relaxation mechanism, i.e., $B1_{ox} \rightleftharpoons B1_{red}$, which is described

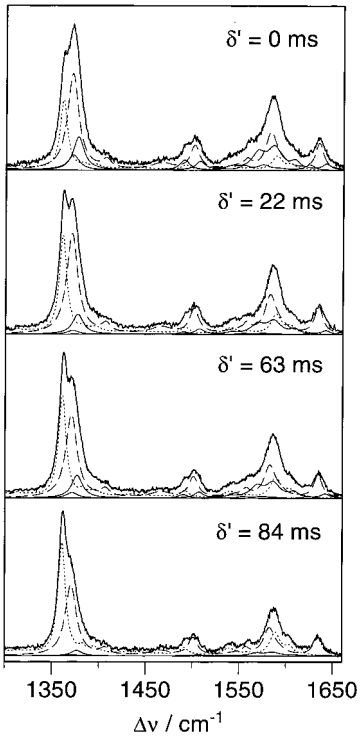

Figure 7. Time-resolved SERR spectra of the adsorbed Cyt-c_{552} for a potential jump from 0.0 to −0.044 V measured at various delay times δ'. The top spectrum is the stationary spectrum measured at 0.0 V. The excitation wavelength was 413 nm. Further experimental conditions are given in the text. The dotted and dashed lines indicate the component spectra of the reduced and oxidized form of state B1, respectively. The solid lines indicate the 6cLS and 5cHS forms of the oxidized state B2.

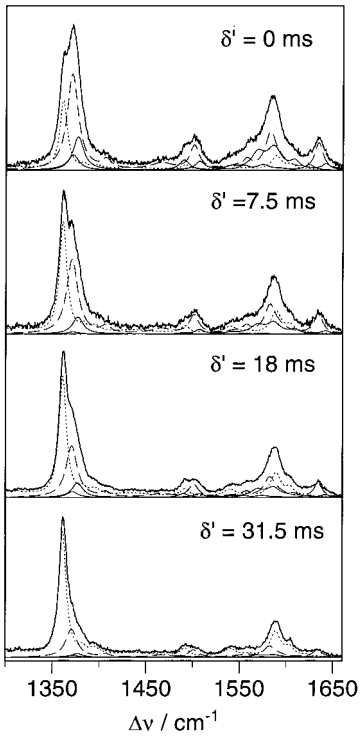

Figure 8. Time-resolved SERR spectra of the adsorbed Cyt-c_{552} for a potential jump from 0.0 to −0.14 V measured at various delay times δ'. The top spectrum is the stationary spectrum measured at 0.0 V. The excitation wavelength was 413 nm. Further experimental conditions are given in the text. The dotted and dashed lines indicate the component spectra of the reduced and oxidized form of state B1, respectively. The solid lines indicate the 6cLS and 5cHS forms of the oxidized state B2.

by eq 5

$$\frac{\Delta c_{\mathrm{B1(red)}}(t=\delta')}{\Delta c_{\mathrm{B1(red)}}(t=0)} = \exp(-(k_1+k_2)t) \qquad (5)$$

with $\delta' = \delta + \Delta t/2$ and k_1 and k_2 referring to the reduction and oxidation of the adsorbed B1, respectively. $\Delta c_{\mathrm{B1(red)}}(t{=}\delta')$ and $\Delta c_{\mathrm{B1(red)}}(t{=}0)$ are given by

$$\Delta c_{\mathrm{B1(red)}}(t{=}\delta') = c_{\mathrm{B1(red)}}(E_{\mathrm{f}}) - c_{\mathrm{B1(red)}}(t{=}\delta') \qquad (6)$$

and

$$\Delta c_{\mathrm{B1(red)}}(t{=}0) = c_{\mathrm{B1(red)}}(E_{\mathrm{f}}) - c_{\mathrm{B1(red)}}(E_i) \qquad (7)$$

where $c_{\mathrm{B1(red)}}(t{=}\delta')$ denotes the actual concentration of $\mathrm{B1_{red}}$ at δ' and $c_{\mathrm{B1(red)}}(E_{\mathrm{f}})$ and $c_{\mathrm{B1(red)}}(E_{\mathrm{i}})$ refer to the equilibrium concentrations at E_{f} and E_{i}, respectively. Because the relative concentration of B1 remains constant during the time-resolved experiments,[30] i.e.,

$$1 = c_{\mathrm{B1(red)}} + c_{\mathrm{B1(ox)}} = f_{\mathrm{B1(red)}} I_{\mathrm{B1(red)}} + f_{\mathrm{B1(ox)}} I_{\mathrm{B1(ox)}} \qquad (8)$$

the equilibrium concentrations of $\mathrm{B1_{red}}$ can be evaluated on the basis of the Nernst equation using eq 8 so that one obtains

$$c_{\mathrm{B1(red)}}(E_{\mathrm{x}}) = \frac{\exp\left(-\frac{nF}{RT}(E_{\mathrm{x}} - E^0)\right)}{1 + \exp\left(-\frac{nF}{RT}(E_{\mathrm{x}} - E^0)\right)} \qquad (9)$$

where E_{x} denotes either the initial or the final potential.

Figure 9 shows the data plotted semilogarithmically according to eq 5 for a selection of potential jumps. The individual data represent average values based on 3−5 series of measurements for each potential jump. In general, the standard deviations for the relative concentrations did not exceed 5%, corresponding to average maximum errors for the logarithmical concentration

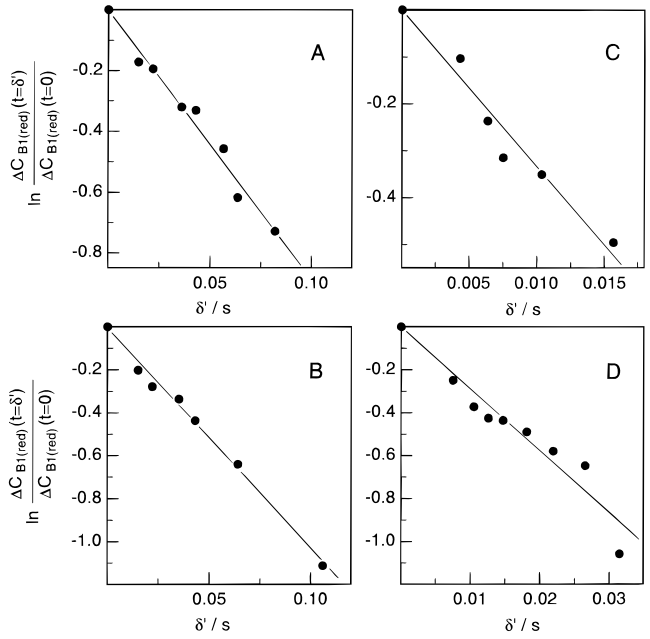

Figure 9. Plots of the concentrations changes of the reduced state B1 as a function of the delay time δ' for various potential jumps according to eq 5: (A) 0.0 → −0.07 V; (B) 0.0 → −0.1 V; (C) −0.04 → −0.18 V; (D) 0.0 → 0.14 V. The data were determined from the time-resolved SERR spectra as described in the text.

TABLE 2: Kinetic Parameters of the Heterogeneous Electron Transfer Reaction of Cyt-c_{552} as Determined by Time-resolved SERR Spectroscopy[a]

k_1 (s^{-1})	$-\Delta E$ (V)	$-\Delta E_{cor}$ (V)	E_f (V)	E_i (V)	σ
4.3	0.0	0.0	−0.044	0.0	0.9624
6.5	0.026	0.024	−0.07	0.0	0.9891
9.2	0.056	0.047	−0.1	0.0	0.9965
18.9	0.076	0.067	−0.12	0.0	0.8937
28.0	0.096	0.086	−0.14	0.0	0.9636
32.5	0.136	0.120	−0.18	−0.04	0.9778
46.6	0.156	0.140	−0.2	−0.04	0.9019
55.0	0.176	0.160	−0.22	−0.04	0.9908

[a] k_1 refers to the unimolecular heterogeneous reduction rate constant. The overpotential, the initial and final potentials of the potential jump experiments, denoted by ΔE, E_i, and E_f, respectively, refer to uncorrected potentials. ΔE_{cor} are the overpotentials corrected for the potential drop at the redox site according to eq 11.

ratio (Figure 9) of 15%. For all potential jumps, the data follow a straight line with good correlations coefficients (>0.96) in most cases.

From the slope m, which is equal to the sum of k_1 and k_2, and the equilibrium constant $K(E_f) = k_1/k_2$ one obtains

$$k_1 = \frac{m}{\left(1 + \frac{1}{K(E_f)}\right)} \tag{10}$$

A complete list of the rate constants determined in this way is given in Table 2. The average error of these rate constants is ca. 12%.

Discussion

Adsorption of Cyt-c_{552}. Cyt-c_{552} exhibits SERR spectra of very strong intensities, which even exceed those observed for Cyt-*c*.[19] These findings suggest that like for Cyt-*c*, the adsorption equilibrium of Cyt-c_{552} is highly exergonic, leading to high concentrations of the adsorbed species.[19,31] On first sight, this observation is surprising, inasmuch as the Cyt-c_{552} lacks the lysine cluster on the front surface of the protein, i.e., around the exposed heme edge.[23] In Cyt-*c* this part of the protein surface serves as the binding domain for negatively charged surfaces such as electrodes covered by a layer of specifically adsorbed anions.[11] In Cyt-c_{552} the exposed heme edge is surrounded by hydrophobic amino acids such as Leu, Val, Ala, and Gly, whereas a cationic binding domain including several lysine residues is located on the backside of the protein, i.e., remote from the exposed heme edge.[23,24] Because efficient binding of Cyt-c_{552} in the electrical double layer requires chloride anions which are specifically adsorbed on the metal surface, it is evident that protein adsorption occurs via electrostatic interactions between the chemisorbed chlorides and the cationic binding domain on the backside of Cyt-c_{552}.[24]

Conformational State B2 of the Adsorbed Cyt-c_{552}. The component spectra of the conformational state B2 of Cyt-c_{552} are similar to those of Cyt-*c*.[12,21] For Cyt-*c*, the structural changes associated with the formation of B2 are restricted to the heme pocket and include the dissociation of the axial methionine (Met-80) ligand from the heme iron.[11,12] In the oxidized state, the sixth-coordination site either remains vacant (5cHS) or is occupied by a new strong ligand providing a 6cLS configuration.[32] For this 6cLS species of B2 the frequencies of the marker bands are unusually high and the relative RR intensities of the modes ν_{10} and ν_2 are drastically altered compared to those of the His/Met-ligated Cyt-*c* in solution or in the adsorbed state B1. In Cyt-c_{552}, the spectral changes in B2 compared to those in B1 are very similar to those of Cyt-*c*, including the substantial upshifts of the marker bands and the characteristic alterations of the relative intensities of ν_{10} and ν_2. Furthermore, for both Cyt-c_{552} and Cyt-*c* the redox potential of the 6cLS form of B2 is substantially shifted to negative values (<−0.3 V).[12,19,33] This comparison suggests that, in the B2 state of both Cyt-c_{552} and Cyt-*c*, the heme iron exhibits the same coordination pattern.

The reduced form of B2 is much less stable in Cyt-c_{552} than in Cyt-*c* because it is readily converted to the reduced B1, thereby restoring the original His/Met ligation pattern. Thus, the 6cLS species of the reduced B2 is only found upon laser-induced heating of the sample (in SERR experiments with nonrotating electrodes) and it cannot be ruled out that the corresponding component spectrum reflects already an His/Met configuration within a structural perturbed heme pocket, i.e., an intermediate state formed during the conversion from the oxidized B2(6cLS) to the reduced B1. In fact, the spectrum does not differ strongly from that of the reduced B1. These findings as well as the lack of a reduced B2 HS species indicate that, particularly in the ferrous form, the B1 state of Cyt-c_{552} exhibits a much higher stability compared to that of Cyt-*c*.[34] This higher stability of the native heme pocket structure in Cyt-c_{552} may be due to the larger separation of the heme site from the binding domain and weaker electrostatic interactions in the electrical double layer and due to the additional C-terminal peptide segment stabilizing the compact protein structure.[23]

Conformational State B1 of the Adsorbed Cyt-c_{552}. The far-reaching similarities between the component spectra of B1 and the RR spectra of the protein in solution demonstrate that in this state the structure of the adsorbed Cyt-c_{552} remains essentially unchanged. There are only minor frequency shifts of less than 1.5 cm^{-1} for some of the bands which may be either due to an electrochemical Stark effect on the vibrational energy levels of the heme or due to subtle alterations of the heme pocket. Again, this observation is in line with previous results for Cyt-*c*.[12] The conservation of the protein structure of Cyt-c_{552} is also reflected by the redox potential of B1 ($E^0 = -0.044$ V) which is similar, albeit not identical, to that of Cyt-c_{552} in solution ($E_s^0 = -0.013$ V).[29] This slightly negative shift can be qualitatively understood in terms of the potential distribution across the electrical double layer. Such effects have been noted previously in electrochemical studies of adsorbed polymers carrying a redox center at a distance d_{RC} relative to the electrode surface.[35,36]

The potential drop E_{RC} at the redox center can be estimated according to the plane-of-electron-transfer (PET) model developed by Smith and White.[35] We have now extended this model to the experimental conditions of the present study by taking into account that Cyt-c_{552} is bound to a layer of specifically adsorbed chloride anions (Appendix I). For E_{RC} as defined by eq 11

$$E_{RC} = E - E_s^0 + \frac{RT}{F} \ln\left(\frac{c_{B1(red)}}{c_{B1(ox)}}\right) \tag{11}$$

The application of Gauss' law to the charge densities and interfacial potentials in the electrical double layer yields

$$E_{RC} = \frac{\sigma_{IH}\epsilon_{RC}d_{IH} + \epsilon_0\epsilon_{RC}\epsilon_{IH}(E - E_{pzc}) + (d_{IH}\epsilon_{RC} + d_{RC}\epsilon_{IH})\sigma_{RC}}{\epsilon_0[\epsilon_{IH}\epsilon_{RC} + (d_{IH}\epsilon_{RC} + d_{RC}\epsilon_{IH})\epsilon_S\kappa]} \tag{12}$$

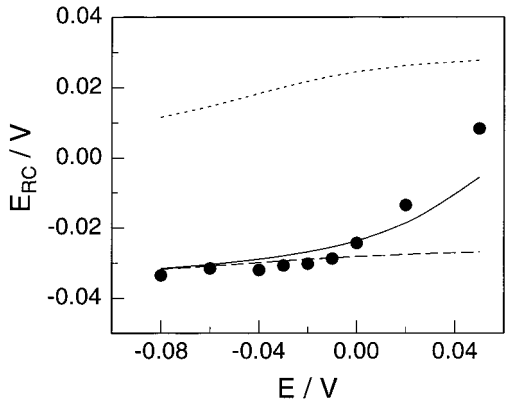

Figure 10. Calculated potential drop at the redox site of the adsorbed Cyt-c_{552} as a function of the applied potential according to eq 12. The solid and dashed lines represent the calculated values with and without taking into account the effect of Ag oxidation on the charge distribution in the inner Helmholtz layer (see Appendix I for further details). The dotted line refers to the original PET model by Smith and White,[35] neglecting specifically adsorbed anions. The experimental values derived from the potential-dependent SERR experiments are represented by circles.

with

$$\sigma_{RC} = e\Gamma_{prot}((z_{red} + 1)(1 - c_{B1(red)}) + z_{red}c_{B1(red)}) \quad (13)$$

where σ_{IH} and ϵ_{IH} are the charge density and dielectric constant in the inner Helmholtz layer (with the thickness d_{IH}) and ϵ_S and ϵ_{RC} are the dielectric constants in the solution and the protein, respectively. The symbols Γ_{prot}, z_{red}, E_{pzc}, and κ denote the particle density of adsorbed protein molecules, the net charge number of the protein, the potential of zero charge, and the Debye length, respectively; e and ϵ_0 have the usual meaning.

Numerical calculations were carried out using the experimental data for the $B1_{red} \rightleftharpoons B1_{ox}$ redox equilibrium as determined from the SERRS experiments in KCl/Tris-HCl solution ($\epsilon_S = 78$). For ϵ_{IH} and ϵ_{RC} we have adopted values of 6 and 2, as suggested for the dielectric constants of the electrical double layer and proteins, respectively.[37,38] For d_{IH} a value of 4 Å (diameter of Cl^-) was assumed, whereas d_{RC} (20 Å), i.e., the distance from the heme center to the putative binding domain, and the diameter (35 Å) of the protein were taken from the crystal structure.[23] This latter value was used to estimate Γ_{prot} by assuming that (as in the case of Cyt-c)[31] only 15% of the total surface is covered by Cyt-c_{552} because protein−protein interactions are likely to prohibit a tighter packing. The model assumes that the only charge in the protein is at the redox site, i.e., at the heme iron ($z_{red} = +2$).[35,39] For E_{pzc}, we have taken a value of −0.97 V, assuming a cancellation of the expected small positive and negative shifts due to adsorption of chloride and the surface roughness, repectively.[40,41] The density of negative charges on the Ag surface (adsorbed Cl^- anions) σ_{IH} was estimated according to a previous study by Hupp et al.[42] and was either taken to be potential-independent in the potential range under consideration or corrected for the oxidation of Ag, i.e., the formation of AgCl ($E^o_{Ag/AgCl} = +0.06$ V).

Figure 10 shows the potential drop E_{RC} calculated as a function of the applied potential according to eq 12. Even when the effect of Ag oxidation (dashed line) is neglected, the model can reproduce the potential shifts determined from the experimental values according to eq 11, except for the most positive potentials (≥+0.02 V). When the neutralization of negative charges due to the formation of AgCl at positive potentials (solid line) are taken into account an increase of E_{RC} at positive potentials is predicted in agreement with the experimental data. In contrast, calculations neglecting the contribution of chemisorbed anions yield positive E_{RC} values in the entire potential range (Figure 10; dotted line), implying that the potential drop at the redox site is controlled by chemisorption of anions, unavoidable in SERS experiments.

The calculations based on the present model (Figure 10; solid line) also provide a satisfactorily quantitative prediction of the experimental results. When the applied electrode potentials are by the calculated E_{RC} values, a Nernstian plot of all the experimental data (i.e., $c_{B1(red)}/c_{B1(ox)}$) between −0.08 and +0.05 V yields a good linear correlation ($\sigma = 0.99$) with a slope corresponding to $n = 0.89$, i.e., close to the theoretical value. The corrected redox potential obtained in this way is −0.015 V, which agrees very well with that determined for Cyt-c_{552} in solution.

In view of the crude underlying assumptions and approximations of the PET model, the quantitative agreement should not be overestimated.[39] Nevertheless, it is obvious that potential drop at the redox site is due to the charge distribution in the electrical double layer.[43] Furthermore, it can be concluded that the true redox potential of the adsorbed B1 is in fact the same as that of the dissolved species, which is expected in view of the structural similarity of Cyt-c_{552} in state B1 and in solution as deduced from the comparison of the SERR and RR spectra.

Kinetics of Electron Transfer and Conformational Transitions. The higher stability of the B1 state of Cyt-c_{552} compared to that of Cyt-c is also reflected by the kinetics of the conformational transitions. Whereas in Cyt-c_{552} the transition of the oxidized B1 to the oxidized B2 at positive potentials is much slower than the ET of B1, the back conversion in the reduced B1 at −0.4 V is very fast so that the kinetics of the ET process of B2 cannot be analyzed. In contrast, Cyt-c exhibits a much slower conformational transition to B1 in the reduced form (at −0.4 V), but the formation of the oxidized B2 at 0.0 V occurs on the same time scale as the $B1_{red} \rightarrow B1_{ox}$ ET reaction.[21,33]

Potential Dependence of the Electron-Transfer Rate Constants. The ET reactions of molecular species at electrodes can be adequately described by Marcus theory, which takes into account the energy distribution of electrons about the Fermi level.[44] Nahir et al.[8] derived a simple expression in which the Fermi−Dirac distribution is replaced by a step function, neglecting the contributions from high and very low energy levels. Thus, the ET rate constant for the heterogeneous reduction of the adsorbed Cyt-c_{552} as a function of the overpotential ΔE is given by

$$k_{ET} = A\frac{\sqrt{\pi\lambda RT}}{F}\left(1 - \mathrm{erf}\frac{F\Delta E + \lambda}{2\sqrt{\lambda RT}}\right) \quad (14)$$

where λ is the reorganization energy. For the formal rate constant at $\Delta E = 0$, $k_{ET,0}$, one obtains

$$k_{ET,0} = A\frac{\sqrt{\pi\lambda RT}}{F}\left(1 - \mathrm{erf}\frac{\lambda}{2\sqrt{\lambda RT}}\right) \quad (15)$$

so that for the ratio $k_{ET}/k_{ET,0}$ (eqs 14 and 15), the constant A cancels, yielding

$$\frac{k_{ET}}{k_{ET,0}} = \frac{1 - \mathrm{erf}\frac{F\Delta E + \lambda}{2\sqrt{\lambda RT}}}{1 - \mathrm{erf}\frac{\lambda}{2\sqrt{\lambda RT}}} \quad (16)$$

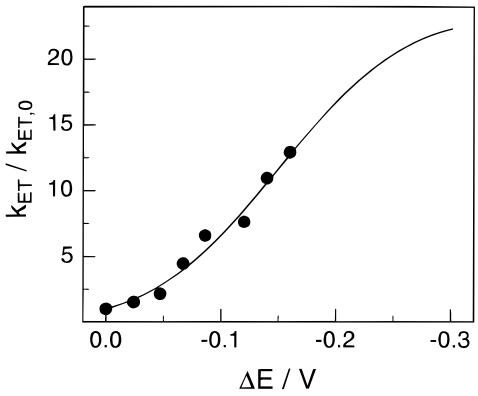

Figure 11. Ratio of the rate constants $k_{ET}/k_{ET,0}$ as a function of the overpotential ΔE_{cor} corrected for the potential drop across the double layer. The solid line represents a least-squares fit of eq 16 to the experimental data taken from Table 2.

A least-squares fit of eq 16 to the experimental data (Table 2) gives a good correlation for $\lambda = 0.15$ eV with a root-mean-square (rms) error of 16% when using the corrected potentials (Figure 11).[45] When the error of the rate constant determination of ca. 12% is taken into acount, the upper and lower limit of λ is estimated to be 0.11 and 0.2 eV. An error analysis reveals that these values are associated with an rms error of 20%, whereas below and above these limits the error substantially increases. A more accurate determination of λ requires measurements at higher driving forces (more negative overpotentials) to reach the plateau of the $k_{ET} = f(\Delta E)$ dependence. These experiments are currently prohibited by the present technical constraints but are, in principle, feasible by the time-resolved SERR spectroscopic method.

The ET reaction of Cyt-c_{552} has not been studied in the past. However, there is a large body of experimental and theoretical data for the reorganization energy of ET reactions of Cyt-*c* in the literature.[3,8,9,38,46,47] The experimental data have been obtained by the analysis of photoinduced ET reactions, where photoactive redox labels were covalently attached on the protein surface,[3] as well as by electrochemical techniques applied to the native protein.[8,9,46] Reorganization energies derived from photoinduced ET reactions are 0.7 eV or higher, depending on the appropriate consideration of the contributions from the redox label (a ruthenium(II) complex). Such effects have not been considered in electrochemical experiments because the reorganization energy of the "redox partner", i.e., the electrode, is zero. Using cyclic voltammetry, Miller and co-workers determined λ to be 0.58, 0.62, and 0.61 eV for Cyt-*c* from horse, tuna, and yeast (iso-1) using cyclic voltametry.[9] These studies refer to the dissolved heme proteins exchanging electrons with a gold electrode covered by a self-assembled monolayer (SAM) of aliphatic ω-hydroxythiols. Therefore, reorganization energies determined in this way include contributions of the structural reorganization of the redox site (λ_{RC}) and the protein (λ_P) as well as of the orientational reorganization of the surrounding solvent molecules (λ_S). The latter contribution can be of the same magnitude as the sum of λ_{RC} and λ_P according to theoretical calculations.[38] Thus, the substantially smaller reorganization energies (0.28−0.34 eV) determined for Cyt-*c* at ω-carboxylthiol-coated Au electrodes[8,46] may be rationalized in terms of a lowering of λ_S because on these SAMs Cyt-*c* is strongly adsorbed so that only a part of the protein remains solvent-exposed. Therefore, a low reorganization energy is not unexpected for Cyt-c_{552} adsorbed on a Ag surface. However, the value obtained in this work (0.15 eV) is even lower than that obtained by Nahir et al. for Cyt-*c* bound to the SAM-modified Au electrode.[8,46]

Comparing kinetic data from SERR spectroscopy and electrochemical techniques, one has to keep in mind that the latter methods cannot distinguish between multiple redox-active forms of the bound heme protein. However, the redox potential found by Nahir et al. is close that of Cyt-*c* in solution[8] so that a coupling with conformational equilibria is not very likely. Thus, both the electrochemical study by these authors and the present SERR spectroscopic study refer to a well-defined state of the adsorbed protein, i.e., the (native) states B1 of Cyt-*c* on the SAM-coated Au electrode and Cyt-c_{552} on the bare Ag electrode, respectively.

On the uncoated electrode, the heme protein is adsorbed on the Helmholtz layer, whereas as on the SAM-coated electrode it is located in the diffuse part of the double layer. In the latter case, the static dielectric constant of the molecular surrounding should be close to that of the bulk solution, but it is much smaller in the Helmholtz layer.[37] Because λ_S is proportional to the difference of the reciprocal optical and static dielectric constants,[38,47] the solvent reorganization energy is expected to be smaller for molecules adsorbed at the inner Helmholtz plane. Then, λ_{RC} and λ_P should give the dominant contribution to the reorganization energy determined for Cyt-c_{552} in the present SERR study.

The inner sphere reorganization energy λ_{RC} is likely to be similar for Cyt-c_{552} and for Cyt-*c*, whereas λ_P may be different for both proteins. For Cyt-*c*, λ_{RC} has been calculated to be 0.13 eV while values of 0.14 and 0.67 eV have been obtained for λ_P depending on the computational method.[38] In view of these calculations, one may conclude that for the adsorbed Cyt-c_{552} the contribution of λ_P to the total reorganization is much smaller compared to that of Cyt-*c*. This conclusion is supported by a comparison of the crystal structures of the oxidized and reduced Cyt-c_{552}, which reveal significantly smaller redox-linked conformational changes than those for Cyt-*c*.[48]

The formal heterogeneous ET rate constant ($\Delta E = 0$ V) for Cyt-c_{552} adsorbed in the Ag/electrolyte interface is comparable to that estimated for yeast iso-1 Cyt-*c* (4.3 vs 3.5 s^{-1}).[21,33] In previous studies rate constants for Cyt-*c* bound to ω-carboxylthiol- and ω-hydroxylthiol-coated Au electrodes that vary from 8000 to 0.21 s^{-1} were measured, depending on the type of the monolayer and the type of Cyt-*c*.[9,10] Inspecting the wide range of values found at these SAM-coated electrodes, it is noted that for comparable chain lengths of the monolayers the rate constants of immobilized Cyt-*c* at ω-carboxylthiol-coated surfaces are substantially lower than those determined at electrodes with ω-hydroxylthiol or mixed ω-hydroxylthiol/ω-carboxylthiol coatings where the binding interactions are much weaker. These discrepancies may reflect a poorer electronic coupling for the electrostatically bound heme proteins possibly due to the charged carboxylate headgroups that might provide an electric field barrier for the ET.

The effect of strong electric fields may also be the reason why the rate constants of Cyt-c_{552} and Cyt-*c* adsorbed at the inner Helmholtz plane are much smaller than those for Cyt-*c* bound to ω-carboxylthiol-coated electrodes.[49] It has been shown that the long-distance charge recombination in photosynthetic reaction centers can be slowed by a factor of ca. 4 when an external electric field of 10^6 V/cm is applied.[50] Similar field strengths exist at the protein binding site of the ω-carboxylthiol monolayers on the metal electrode. However, in the Helmholtz double layer, particularly in the presence of chemisorbed anions, the electric field strength may be higher by more than a factor

of 10, which may account for the slower ET rates determined in the SERR experiments. Note that Cyt-*c* immobilized on a *N*-acetylcysteine-coated Au electrode exhibits a similarly low ET rate constant (3.4 s^{-1}),[7] which may be due to opposing effects: a weaker electric field favoring the ET and a larger distance to the electrode slowing down the ET compared to the directly adsorbed heme protein.[51]

Implications for the Biological ET Process. For the reaction of Cyt-*c* with CcO, the interprotein ET process from heme *c* to the binuclear copper center proceeds with a rate constant of ca. 6×10^4 s^{-1}.[52] Because the turnover numbers from steady-state kinetic measurements for this protein couple and for Cyt-c_{552}/ba_3-oxidase are of the same of order of magnitude,[22,53] it is likely that also the interprotein ET rate constant of Cyt-c_{552} is comparable to that of Cyt-*c*. Thus, one may assume that the natural ET of Cyt-c_{552} occurs much faster than the heterogeneous ET at the Ag electrode. In the biological process, Cyt-c_{552} most likely binds to the ba_3-oxidase via the unpolar binding domain close to the heme pocket so that the intraprotein ET distance is much shorter (7 Å) compared to that of the ET at the electrode where Cyt-c_{552} binds via the positively charged interaction domain that corresponds to an intraprotein ET distance of 20 Å.[24] Although the total distance to the primary electron acceptor in the ba_3-oxidase is not yet known, it may well be that both a shorter ET pathway as well as the lack of a negatively charged interface (as discussed above) account for the faster biological ET rate.

The conformational transition to state B2 of the adsorbed Cyt-c_{552} was found to be much slower than the ET rate of B1, even in the electrochemical system. Therefore, it is not very likely that this conformational transition occurs upon complex formation with the ba_3-oxidase during the biological redox process. In fact, the RR spectroscopic analysis of the (nonreactive) fully oxidized Cyt-c_{552}/ba_3-oxidase complex reveals no contribution of B2.[25] Consequently, Cyt-c_{552} reveals a different behavior compared to Cyt-*c* which in the complex with CcO exists in an equilibrium between the states B1 and B2.[13] In contrast to the Cyt-c_{552}/ba_3-oxidase couple, the Cyt-*c*/CcO complex is formed via electrostatic interactions, which in turn have been shown to be essential for inducing the conformational transition.[13c] Furthermore, it was found that on the Ag electrode the conformational transition to the oxidized B2 is even faster (ca. 8 s^{-1}) than the formal heterogeneous rate constant for the ET of B1 (ca. 3.5 s^{-1}), supporting the view of conformational control of the interprotein ET.[13c,21,33]

Such a complex ET process can be ruled out for Cyt-c_{552}. It is tempting to attribute this mechanistic difference compared to Cyt-*c* to the more stable protein structure brought about by the additional peptide segment that wraps around the remainder of the protein.[23] This higher protein stability can be interpreted in terms of an adaptation to the extreme living conditions at temperatures >70 °C of *Th. thermophilus*. The additional peptide segment is also involved in constituting the atypical hydrophobic binding domain, which in turn accounts for the specificity of the ET reaction to the ba_3-oxidase. Because the reduced structural flexibility of Cyt-c_{552} does not allow conformational control of the biological redox process, a high efficiency of the interprotein ET may be achieved by optimizing the heme pocket structure in such a way that only minimal structural changes are associated with the ET.[48] The unusual low reorganization energy determined in this work appears to support this idea.

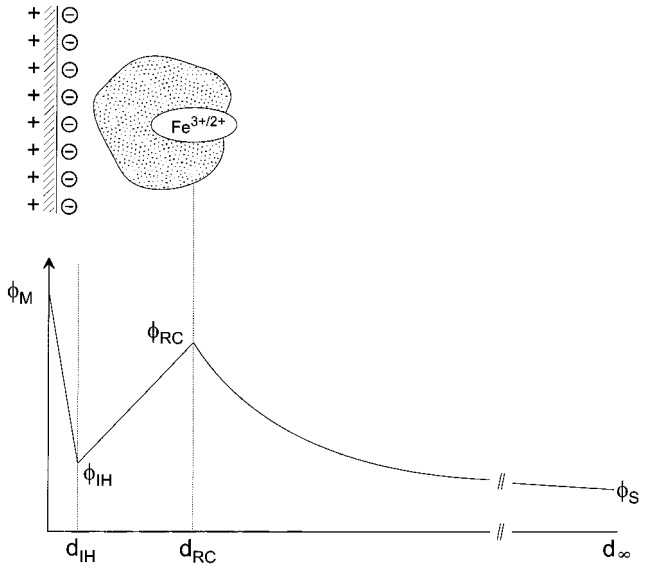

Figure 12. Schematic representation of the modified PET model based on the original model from Smith and White.[35]

Conclusions

The results of the present study provide a comprehensive picture about the heterogeneous ET process of Cyt-c_{552}. The specificity of the ET dynamics and mechanism of this heme protein can be explained in terms of its unique structural properties compared to those of other *c*-type cytochromes. Furthermore, it has been shown that strong electric fields in the electrical double layer of electrodes may have a substantial impact on heterogeneous redox processes. The comparison of the kinetic results obtained for immobilized cytochromes in the present study and in previous studies suggests that the heterogeneous ET is controlled by an interplay of electric field effect and distance dependence. In addition, the interfacial redox processes may be associated with structural changes of the redox-active species prior to or after the ET step. It is the main advantage of time-resolved SERR spectroscopy compared to conventional electrochemical methods that it is capable to disentangle such complex interfacial reactions. In many cases the natural long-range ET of heme proteins occur at charged interfaces and, hence, are subject to electric field strengths similar to those at electrodes. Therefore, not only does the present SERR spectroscopic study contribute to a better understanding of the structure−function relationship of Cyt-c_{552} but the results also are of relevance in the wider context of biological long-range ET reactions in general.

Acknowledgment. The work was supported by the Deutsche Forschungsgemeinschaft (Hi 464/4-1; 464/4-2; to P.H.). The authors wish to thank Professors K. Schaffner and G. Buse for support and continuous encouragement. P.H. is a recipient of a Heisenberg fellowship by the Deutsche Forschungsgemeinschaft, which is gratefully acknowledged. The authors wish to thank B. Deckers for technical assistance.

Appendix I

An expression for the actual potential at the redox site of the adsorbed protein is derived by a modification of the PET model developed by Smith and White.[35] This modification takes into account that the protein is not adsorbed directly on the metal surface but bound to a layer of specifically adsorbed anions (Figure 12). Furthermore, the redox site is assumed to be in contact with the solvent. This approximation appears to be

justified for Cyt-c_{552} in view of the exposed heme edge. The potential drop E_{RC} at the redox center RC is given by the modified Nernst equation (A1) for the one-electron-transfer couple $B1_{red} \rightleftharpoons B1_{ox}$,

$$E_{RC} = E - E_S^0 + \frac{RT}{F} \ln\left(\frac{c_{B1(red)}}{c_{B1(ox)}}\right) \quad \text{(A1)}$$

whereas E_s^0 is the redox potential in solution and E_{RC} is given by

$$E_{RC} = \phi_{RC} - \phi_S \quad \text{(A2)}$$

with ϕ_{RC} and ϕ_S denote the potentials at the RC and in the bulk solution. The relationships between the individual interfacial potentials ϕ_M, ϕ_{IH}, ϕ_{RC}, and ϕ_S, and the charge densities ϕ_M, ϕ_{IH}, ϕ_{RC}, and ϕ_S in the different segments of the interface (defined by d_{IH}, d_{RC}, and d_∞; see Figure 12) are obtained by applying Gauss' law:

$$\sigma_M = \frac{\epsilon_0\epsilon_{IH}}{d_{IH}}(\phi_M - \phi_{IH}) \quad \text{(A3)}$$

$$\sigma_M + \sigma_{IH} = \frac{\epsilon_0\epsilon_{RC}}{d_{RC}}(\phi_{IH} - \phi_{RC}) \quad \text{(A4)}$$

$$\sigma_{RC} = e\Gamma_{prot}((z_{red} + 1)(1 - c_{B1(red)}) + z_{red}c_{B1(red)}) \quad \text{(A5)}$$

$$\sigma_S = -\epsilon_0\epsilon_S\kappa\frac{2kT}{e}\sinh\left(\frac{e}{2kT}(\phi_{RC} - \phi_S)\right) \quad \text{(A6)}$$

Finally, charge neutrality must be fulfilled according to

$$\sigma_M + \sigma_{IH} + \sigma_{RC} + \sigma_S = 0 \quad \text{(A7)}$$

In eqs A3−A6 the constants ϵ_0, e, and k have the usual meaning, ϵ_{IC}, ϵ_{RC}, and ϵ_S are the dielectric constants of the inner Helmholtz layer, the protein, and the bulk solution, and κ is the Debye length. The particle density Γ_{prot} refers to the total number of protein molecules per area and $c_{B1(red)}$ denotes the fraction of the reduced B1 species with the net charge number of z_{red}.

After combination with eq A3, eq A6 can be linearized (for small E_{RC}) and one obtains

$$\sigma_S = -\epsilon_0\epsilon_S\kappa E_{RC} \quad \text{(A8)}$$

The error associated with this approximation is ca. 5% for $E_{RC} = 30$ mV and, hence, is acceptable for the estimations of this approach. The charge density in the inner Helmholtz layer σ_{IH} results from the specifically adsorbed anions. Upon approach to the oxidation potential of Ag, E_{Ag}^0, the formation of Ag^+ leads to a (partial) compensation of the negative charges according to

$$\sigma_{IH}(E) = \frac{\sigma_{IH}(\text{n.F.})}{1 + \exp\left(-\frac{F}{RT}(E - E_{Ag}^0)\right)} \quad \text{(A9)}$$

where σ_{IH}(n.F.) refers to the adsorbed anions in the non-Faradayic region as determined by capacitance measurements.[42] When the relationships for the electrode potential E and the potential at zero charge E_{pzc} are used,

$$E = \phi_M - \phi_{ref} \quad \text{(A10)}$$

$$E_{pzc} = \phi_S - \phi_{ref} \quad \text{(A11)}$$

where ϕ_{ref} is the reference potential, a combination of eqs (A2), (A3), (A4), (A7), and (A8) leads to

$$E_{RC} = \frac{\sigma_{IH}\epsilon_{RC}d_{IH} + \epsilon_0\epsilon_{RC}\epsilon_{IH}(E - E_{pzc}) + (d_{IH}\epsilon_{RC} + d_{RC}\epsilon_{IH})\sigma_{RC}}{\epsilon_0[\epsilon_{IH}\epsilon_{RC} + (d_{IH}\epsilon_{RC} + d_{RC}\epsilon_{IH})\epsilon_S\kappa]} \quad \text{(A12)}$$

which allows one to determine the potential drop at the redox center of the adsorbed Cyt-c_{552} (see eq A1).

References and Notes

(1) (a) Isied, S. S. *Prog. Inorg. Chem.* **1984**, *32*, 443. (b) Williams, R. J. P. *Mol. Phys.* **1989**, *68*, 1. (c) Bowler, B. E.; Raphael, A. L.; Gray, H. B. *Prog. Inorg. Chem.* **1990**, *38*, 259. (d) Johnson, M. K., King, R. B., Kurtz, D. M., Kutal, C., Norton, M. L., Scott, R. A., Eds. *Adv. Chem. Ser.* **1990**, *226*. (e) Bolton, J. R., Mataga, N., Mclendon, G., Eds. *Adv. Chem. Ser.* **1991**, *228*. (f) Gray, H. B.; Ellis, W. R., Jr. In *Bioinorganic Chemistry*; Bertini, I., Gray, H. B., Lippard, S. J., Valentine, J. S., Eds.; University Science Books: Mill Valley, CA, 1994; p 315.

(2) (a) Pettigrew, G. W.; Moore, G. R. *Cytochrome c—Biological Aspects*; Springer-Verlag: Berlin, 1987. (b) Scott, R. A., Mauk, A. G., Eds. *Cytochrome c*—A *Multidisciplinary Approach*; University Science Books: Sausalito, CA, 1995.

(3) Scott, R. A. In *Cytochrome c*—A *Multidisciplinary Approach*; Scott, R. A., Mauk, A. G., Eds.; University Science Books, Sausalito, CA, 1995; p 515.

(4) Watkins, J. A.; Cusanovich, M. A.; Meyer, T. E.; Tollin, G. *Protein Sci.* **1994**, *3*, 2104.

(5) (a) Bowden, E. F.; Hawkridge, F. M.; Blount, H. N. In *Comprehensive Treatise of Electrochemistry*; Srinivasan, S., Chiznadzhiev, Yu., Bockris, J. O'M., Convay, B., Yeager, E., Eds.; Plenum Press: New York, 1985; Vol. 10, p 297. (b) Bond, A. M.; Hill, H. A. O. In *Metal Ions in Biological Systems*; Sigel, H., Sigel, A., Eds.; Marcel Dekker: New York, 1991; Vol. 27, p 431.

(6) Albery, W. J.; Eddowes, M. J.; Hill, H. A. O.; Hillman, A. R. *J. Am. Chem. Soc.* **1981**, *103*, 3904.

(7) Cooper, J. M.; Greenough, K. R.; McNeil, C. J. *J. Electroanal. Chem.* **1993**, *347*, 267.

(8) (a) Nahir, T. M.; Clark, R. A.; Bowden, E. F. *Anal. Chem.* **1994**, *66*, 2595. (b) Nahir, T. M.; Bowden, E. F. *J. Electroanal. Chem.* **1996**, *410*, 9.

(9) (a) Terretaz, S.; Cheng, J.; Miller, C. J. *J. Am. Chem. Soc.* **1996**, *118*, 7857. (b) Cheng, J.; Terretaz, S.; Blankman, J. I.; Miller, C. J.; Dangi, B.; Guiles, R. D. *Isr. J. Chem.* **1997**, *37*, 259.

(10) El Kasmi, A.; Wallace, J. M.; Bowden, E. F.; Binet, S. M.; Linderman, R. J. *J. Am. Chem. Soc.* **1998**, *120*, 225.

(11) Hildebrandt, P. In *Cytochrome c*—A *Multidisciplinary Approach*; Scott, R. A., Mauk, A. G., Eds.; University Science Books: Sausalito, CA, 1995; p 285.

(12) Hildebrandt, P.; Stockburger, M. *Biochemistry* **1989**, *28*, 6710.

(13) (a) Hildebrandt, P.; Heimburg, T.; Marsh, D.; Powell, G. L. *Biochemistry* **1990**, *29*, 1661. (b) Hildebrandt, P.; Vanhecke, F.; Buse, G.; Soulimane, T.; Mauk, A. G. *Biochemistry* **1993**, *32*, 10912. (c) Döpner, S.; Hildebrandt, P.; Rosell, F. I.; Mauk, A. G.; von Walter, M.; Buse, G.; Soulimane, T. *Eur. J. Biochem.* **1999**, *261*, 379.

(14) (a) Bechtold, R.; Kuehn, C.; Lepre, C.; Isied, S. *Nature* **1986**, *322*, 286. (b) Hoffman, B. M.; Ratner, M. R. *J. Am. Chem. Soc.* **1987**, *109*, 6237. (c) Brunschwig, B. S.; Sutin, N. *J. Am. Chem. Soc.* **1989**, *111*, 7454. (d) Feitelson, J.; McLendon, G. *Biochemistry* **1991**, *30*, 5051. (e) Pudlak, M. *J. Chem. Phys.* **1998**, *108*, 5621. (f) Durham, B.; Fairris, J. L.; McLean, M.; Millet, F.; Scott, J. R.; Sligar, S. G.; Willie, A. *J. Bioenerg. Biomembr.* **1995**, *27*, 331.

(15) (a) Chang, R. K.; Laube, B. E. *CRC Crit. Rev. Solid State Mater. Sci.* **1984**, *12*, 1. (b) Smith, W. E. In *Methods of Enzymology*; Riordan, J. F., Vallee, B. L., Eds.; Academic Press: San Diego, CA, 1993; Vol. 226, Part C, p 482.

(16) Cotton, T. M.; Schultz, S. G.; Van Duyne, R. P. *J. Am. Chem. Soc.* **1980**, *102*, 7962.

(17) Niaura, G.; Gaigalas, A. K.; Vilker, V. L. *J. Electroanal. Chem.* **1996**, *416*, 167.

(18) (a) Hobara, D.; Niki, K.; Cotton, T. M. *Dengi Kagaku* **1993**, *61*, 776. (b) Hobara, D.; Niki, K.; Zhou, C.; Chumanov, G.; Cotton, T. M. *Colloids Surf.* **1994**, *93A*, 241. (c) Hobara, D.; Niki, K.; Cotton, T. M. *Biospectroscopy* **1998**, *4*, 161.

(19) Lecomte, S.; Wackerbarth, H.; Hildebrandt, P.; Soulimane, T.; Buse, G. *J. Raman Spectrosc.* **1998**, *29*, 687.

(20) Lecomte, S.; Wackerbarth, H.; Soulimane, T.; Buse, G.; Hildebrandt, P. *J. Am. Chem. Soc.* **1998**, *120*, 7381.

(21) Wackerbarth, H.; Klar, U.; Günther, W.; Hildebrandt, P. *Appl. Spectrosc.* **1999**, *53*, 283.
(22) Soulimane, T.; von Walter, M.; Hof, P.; Than, M. E.; Huber, R.; Buse, G. *Biochem. Biophys. Res. Commun.* **1997**, *237*, 572.
(23) Than, M. E.; Hof, P.; Huber, R.; Bourenkov, G. P.; Bartunik, H. D.; Buse, G.; Soulimane, T. *J. Mol. Biol.* **1997**, *271*, 629.
(24) Lecomte, S.; Hilleriteau, C.; Forgerit, J. P.; Revault, M.; Hildebrandt, P.; Baron, M.-H.; Soulimane, T. Manuscript in preparation.
(25) Gerscher, S.; Hildebrandt, P.; Buse, G.; Soulimane, T. *Biospectroscopy* **1999**, in press.
(26) Döpner, S.; Hildebrandt, P.; Mauk, A. G.; Lenk, H.; Stempfle, W. *Spectrochim. Acta* **1996**, *51A*, 573.
(27) Parthasarathi, N.; Hansen, C.; Yamaguchi, S.; Spiro, T. G. *J. Am. Chem. Soc.* **1987**, *109*, 3865.
(28) Hu, S.; Morris, I. K.; Singh, J. P.; Smith, K. M.; Spiro, T. G. *J. Am. Chem. Soc.* **1993**, *115*, 12446.
(29) Hon-Nami, K.; Oshima, T. *J. Biochem. (Tokyo)* **1977**, *82*, 769.
(30) The adsorption constant of Cyt-c_{552} increases with decreasing potentials so that under equilibrium conditions the amount of adsorbed $B1_{red}$ is higher at -0.2 V than at -0.1 V. However, the adsorption process of Cyt-c_{552} is diffusion-controlled and occurs in the long millisecond range[33] whereas the dwell times at E_f in this potential range are much shorter. Thus, the adsorption equilibrium is not established in the time-resolved experiments so that in a good approximation the amount of adsorbed B1 can be regarded as constant.
(31) Hildebrandt, P.; Stockburger, M. *J. Phys. Chem.* **1986**, *90*, 6017.
(32) Döpner, S.; Hildebrandt, P.; Rosell, F. I.; Mauk, A. G. *J. Am. Chem. Soc.* **1998**, *120*, 11246.
(33) Wackerbarth, H.; Hildebrandt, P., unpublished results.
(34) Also in the oxidized form, the relative stability of B1 with respect to B2 appears to be higher for Cyt-c_{552} than for Cyt-*c*.
(35) Smith, C. P.; White, H. S. *Anal. Chem.* **1992**, *64*, 2398.
(36) Creager, S. E.; Weber, K. *Langmuir* **1993**, *9*, 844.
(37) Bockris, J. O'M.; Reddy, A. K. N. *Modern Electrochemistry*; Plenum Press: New York, 1970; Vol. 2.
(38) Basu, G.; Kitao, A.; Kuki, A.; Go, N. *J. Phys. Chem. B* **1998**, *102*, 2085.
(39) The model neglects additional charges in the protein. However, the qualitative agreement with the experimental results is not affected by assuming values for z_{red} greater than $+2$.
(40) Shlepakov, A. V.; Sevast'yanov, E. S. *Elektrokhimiya* **1978**, *14*, 243.
(41) Valette, G.; Hamelin, A. *J. Electroanal. Chem. Interface Sci.* **1973**, *45*, 301.
(42) Hupp, J. T.; Larkin, D.; Weaver, M. J. *Surf. Sci.* **1983**, *125*, 429.
(43) For Cyt-*c* in solution, a negative shift of the redox potential was found to occur upon specific binding of chloride (Gopal, D.; Wilson, G. S.; Earl, R. A.; Cusanovich, M. A. *J. Biol. Chem.* **1988**, *263*, 11652). However, the shifts reported by these authors are distinctly smaller than that observed for the heterogeneous redox process of Cyt-c_{552} in the present work. Moreover, anion binding cannot account for the nonlinearity of the Nernstian plot at positive potentials which, in contrast, is readily understood on the basis of the present PET model. In addition, this model may also explain (in part) errors associated with the ET rate constant determination. It may be that repetitive potential jumps cause irreversible changes of the charge distribution in the electrical double layer which in turn affect the potential drop at the redox site and thus the ET rate.
(44) (a) Marcus, R. A. *J. Chem. Phys.* **1965**, *43*, 679. (b) Chidsey, C. E. D. *Science* **1991**, *251*, 919.
(45) With the potential drop at the redox site according to eq 11 (cf. Appendix I) being taken into account, corrected values for E_f were obtained which together with the corrected redox potential (-0.015 V) give ΔE_{cor} as listed in Table 2. Using the uncorrected potentials, the reorganization energy was only slightly lower (0.13 eV) but the rms was worse.
(46) Song, S.; Clark, R. A.; Bowden, E. F.; Taylor, M. J. *J. Phys. Chem.* **1993**, *97*, 6564.
(47) Churg, A. K.; Weiss, R. M.; Warshel, A.; Takano, T. *J. Phys. Chem.* **1983**, *87*, 1683.
(48) Than, M. E.; Soulimane, T.; Huber, R. Unpublished results.
(49) The literature data were corrected for the distance dependence using an exponential attenuation factor β of 1.05 $Å^{-1}$.[9a]
(50) Franzen, S.; Boxer, S. G. *Adv. Chem. Ser.* **1991**, *228*, 9.
(51) It is not likely that the ET depends on the kind of the electrode material (Au vs Ag) because relatively fast ETs (at $\Delta E = 0$ V) have been found for (unbound) Cyt-*c* at bare Ag electrodes [$(2.8 \times 10^{-4})-(2.2 \times 10^{-3})$] cm/s; Reed, D. E.; Hawkridge, F. M. *Anal. Chem.* **1987**, *59*, 2334) which compare well with those for SAM-coated Au electrodes [$(1.0 \times 10^{-3})-(1.4 \times 10^{-3})$ cm/s).[9a] On the other hand, a very small value (ca. 3 s^{-1}) was found for Cyt-*c* adsorbed on a tin oxide electrode (Willit, J. L.; Bowden, E. F. *J. Electroanal. Chem.* **1987**, *221*, 265) that is comparable to the constants for Cyt-*c* and Cyt-c_{552} determined by SERR spectroscopy.
(52) Geren, L. M.; Beasley, J. R.; Fine, B. R.; Saunders: A. J.; Hibdon, S.; Pielak, G. J.; Durham, B.; Millett, F. *J. Biol. Chem.* **1995**, *270*, 2466.
(53) Soulimane, T.; Buse, G. *Eur. J. Biochem.* **1995**, *227*, 588.